JOURNAL OF Materials CHEMISTRY

Rapid, energetic metathesis routes to crystalline metastable phases of zirconium and hafnium dioxide

Edward G. Gillan*[a] and Richard B. Kaner*[b]

[a]*Department of Chemistry and the Optical Science and Technology Center, University of Iowa, Iowa City, Iowa, 52242-1294, USA*
[b]*Department of Chemistry and Biochemistry and the Exotic Materials Institute, University of California, Los Angeles, California, 90095-1569, USA*

Received 5th March 2001, Accepted 28th March 2001
First published as an Advance Article on the web 5th June 2001

Rapid, exothermic metathesis (exchange) reactions between $ZrCl_4$ and Na_2O result in crystalline ZrO_2 in seconds. Thermal analysis and *in situ* reaction temperature measurements show that the reaction initiates near the sublimation point of $ZrCl_4$, rapidly reaches temperatures above 1350 °C, and generates a molten NaCl flux for a few seconds. Powder X-ray diffraction demonstrates that the product is a mixture of room-temperature monoclinic and high-temperature cubic ZrO_2 phases. The addition of cubic phase stabilizers such as Ca, Y, or Ce oxides or their chlorides to the reaction results in an increase in cubic phase formation up to nearly 70%. These partially stabilized products can withstand annealing to 1300 °C, unlike the unstabilized product, which reverts to the thermodynamic room-temperature monoclinic form on heating to 900 °C. The analogous reaction between $HfCl_4$ and Na_2O results in crystalline HfO_2. The addition of CaO to this reaction also enhances cubic phase formation.

Introduction

Refractory transition-metal oxides are an industrially important class of ceramic materials.[1] One such ceramic is zirconia, ZrO_2, which is hard, possesses a high melting point (2710 °C), and is resistant to chemical attack by strong acids.[2] Zirconia is also stable in oxidizing environments, allows oxygen diffusion through its bulk,[3] exhibits good thermal conductivity, and is electrically insulating. These properties enable zirconia to be used as an abrasive, as a hard resistant coating for cutting tools, in oxygen electrodes and sensors, and in high-temperature engine components.[1,4] One problem associated with high-temperature structural uses is that zirconia experiences a detrimental volume decrease at 1205 °C associated with a martensitic phase transformation from the room-temperature monoclinic structure (m-ZrO_2) to the higher temperature tetragonal form (t-ZrO_2).[2] This transformation results in a volume change of approximately 5% and can cause cracking and failure in ceramic parts. At even higher temperatures a cubic phase (c-ZrO_2) exists that is stable from 2380 °C to its melting point at 2710 °C. Since the cubic and tetragonal forms of ZrO_2 are structurally very similar and both are related to the fluorite unit cell, this high-temperature phase change presents less of a problem.

Traditionally ZrO_2 has been synthesized from the high-temperature decomposition of zirconium compounds such as nitrates, carbonates, or silicates.[1,2,5] In recent years low-temperature synthetic methods have been developed including aqueous reactions where amorphous zirconium oxide hydrates are precipitated from basic solutions of dissolved zirconium salts such as $ZrCl_4$, $ZrO(NO_3)_2$,[6] or $ZrOCl_2$.[7] These amorphous colloidal precipitates must then be sintered at high temperatures to produce crystalline ZrO_2. The hydrolysis of zirconium alkoxides (sol–gel) has also been successful in preparing zirconia powders and gels.[8] In solution reactions, initial calcination often results in the crystallization of metastable tetragonal or cubic structures. Experimental conditions (*e.g.*, pH, precipitation rate, and precursors) appear to affect the stability of these higher temperature phases with conversion to the room-temperature monoclinic phase occurring from 350 to 700 °C.[6a,7a,9,10] Various studies suggest that t-ZrO_2 formed from precipitation reactions remains stable on heating until the particles reach a critical size (*ca.* 30 nm) and surface free energy favors the transformation to m-ZrO_2.[7a,11]

Combustion reactions can be used to produce metal oxides using reactive precursors based on citrate–nitrate gels[12] and other organic fuels.[13] Metathesis (exchange) reactions between solid precursors have also successfully produced metal oxides in moderate temperature reactions (< 600 °C) along with alkali metal phosphate[14] or halide[15] byproducts. The above routes have advantages over precipitation routes in that they are performed in the solid-state, do not require any outside source of oxygen (*e.g.* H_2O or O_2), and generally result in crystalline products.

Recently, rapid solid-state metathesis (SSM) reactions using metal halides have proven to be quite successful in the chemical synthesis of a wide variety of crystalline refractory materials including borides,[16] nitrides,[17] boron nitride,[18] and oxides.[19] Upon initiation, these reactions reach high temperatures (> 1000 °C) in a fraction of a second and cool very quickly (< 5 s).[20] The rapid nature of these reactions allows for only brief nucleation and growth, resulting in small crystallites and occasionally the formation of metastable phases. For example, the reaction between $ZrCl_4$ and Na_3P produces the high-temperature cubic phase of ZrP, which is the first phase to nucleate and is rapidly quenched to room temperature.[21]

There has been extensive research on the stabilization of high-temperature cubic ZrO_2 to room temperature by addition of small amounts (*ca.* 5–20 at%) of a cubic oxide.[2] Even though t-ZrO_2 and c-ZrO_2 cannot be quenched to room temperature,[22] high-temperature solid-state reactions, solution precipitations, or sol–gel reactions forming ZrO_2 with CaO,[23] Y_2O_3,[24] or CeO_2[25] additions have all been successful in stabilizing these high-temperature phases to room temperature. In these cases, the products are either a mixture of the cubic or tetragonal phase and the monoclinic phase [partially stabilized zirconia (PSZ)] or single-phase stabilized ZrO_2. The concentration of the added oxide determines the amount and phase of the stabilized structure.[23b,24b] The HfO_2 phase diagram and

DOI: 10.1039/b102234m

structural transitions are very similar to those of ZrO_2 and its high-temperature structures also can be stabilized through the formation of solid-solutions with other metal oxides.[26] The tetragonal phase transition for HfO_2 (1670 °C) is higher than ZrO_2, however, making it more difficult to obtain unstabilized high-temperature phases of HfO_2.[27]

The following study describes the successful use of rapid SSM reactions in the synthesis of crystalline cubic ZrO_2. This metastable phase thermally converts to the room-temperature monoclinic phase on heating above 900 °C. The addition of stabilizing agents to the ZrO_2 reaction mixture in the form of metal oxides or metal chlorides increases the amount and stability of the high-temperature cubic phase. SSM reactions are also shown to produce metastable cubic HfO_2.

Experimental

Metathesis reactions

The starting materials were used as received and obtained as follows: Na_2O (Aldrich, 99.7%), Na_2O_2 (Alfa Aesar, 98%), $ZrCl_4$ (Aldrich, 99.5%) and $HfCl_4$ (Alfa Aesar, 98+%, <3% Zr), $CaCl_2$ (Aldrich, tech. grade), $CeCl_3$ (Aldrich, 99.9%), YCl_3 (Aldrich, 99.99%), CaO (Alfa Aesar, 99.95%), CeO_2 (Alfa Aesar, 99.9%), and Y_2O_3 (Alfa Aesar, 99.9%).

The reactant mixtures typically consisted of 1.0 g (4.3 mmol) of $ZrCl_4$ and 0.532 g (8.6 mmol) of Na_2O. Na_2O_2 was also examined as an alternative oxygen source. In all cases, the amounts of reactants were salt-balanced such that there was no excess sodium or chloride. The precursors were ground together with a mortar and pestle in a helium-filled glovebox (Vacuum Atmospheres MO-40) and transferred to a stainless steel reaction vessel modeled after a bomb calorimeter. Reaction ignition was accomplished by a short (<2 s) local initiation from a heated nichrome filament in an argon-filled glovebag. All products were washed with ethanol, followed by 2 M HCl to dissolve any unreacted starting materials and the byproduct salt, and finally rinsed with water and dried. Overall chemical yields were about 50%. In phase stabilization reactions the metal oxides or halides were added to produce a Zr : M molar ratio of 10 : 1 (9 at%). These additives were ground together with the $ZrCl_4$–$2Na_2O$ mixture and the metal halides were salt balanced with an additional amount of Na_2O. Note that the acid wash will dissolve away any unreacted CaO or Y_2O_3, but CeO_2 is only sparingly soluble in acids. **WARNING:** Solid-state metathesis reactions are often very exothermic and may be initiated on grinding reagents together or by addition of a small amount of solvent. Care should be taken to perform reactions of this type on a small scale using precautions afforded to similarly energetic reactions.

Product characterization

Differential scanning calorimetry (DSC-TA Instruments 2910) was performed on a small amount (~10 mg) of the $ZrCl_4$–$2Na_2O$ mixture. The sample was sealed in an aluminium pan and heated at 10 °C min^{-1} in flowing argon. High-temperature differential thermal analysis (DTA-TA Instruments 1600 or Seiko TG/DTA 6300) was run on 15–20 mg samples heated in air at 20 °C min^{-1} in the range of 400–1450 °C. *In situ* reaction temperature measurements were performed in a modified reactor equipped with a 0.1 mm chromel–alumel thermocouple. The thermocouple voltage changes were recorded (*ca.* 40 ms intervals) with a computer-interfaced Hewlett-Packard 34401A multimeter and converted to temperatures using HP Benchlink software. Scanning electron microscopy (SEM: Hitachi S4000 field emission system) and energy dispersive spectroscopy (EDS: EDAX Kevex Quantum system) provided morphological and semi-quantitative compositional information (ZAF method).

The phase and crystallinity of the products were analyzed by powder X-ray diffraction (XRD) using a Siemens D5000 system. A crystalline silicon standard and 0.05 degree increments were used for lattice parameter calculations and crystallite size measurements. Lattice parameters were determined using least squares refinement. The Scherrer and Warren equations[28] were used to calculate average crystallite sizes. High angle XRD was performed in 0.02 degree increments and 10 second count times and the background was smoothed using the Siemens Diffrac-plus EVA program. The simulated patterns were generated using PowderCell 2.3 (www.bam.de/a_v/v_1/powder/e_cell.html). For phase composition purposes the important diagnostic XRD peaks are the $(11\bar{1})_m$ and $(111)_m$ monoclinic reflections at 28.5 and 31.5°, respectively, and the $(111)_{c/t}$ cubic or tetragonal peak at 30.2°. Since the tetragonal phase has lattice parameters that are only slightly distorted from a cubic structure ($c/a = 1.02$), the c-ZrO_2 and t-ZrO_2 peaks overlap at low angles, thus the peak at 30.2° will be referred to as c/t-ZrO_2. The volume fraction of the c/t-ZrO_2 phase ($f_{c/t}$) is approximated using the following relation:[29]

$$f_{c/t} = \frac{I(111)_{c/t}}{I(111)_m + I(11\bar{1})_m + I(111)_{c/t}} \quad (1)$$

where intensity (I) corresponds to the XRD peak area. The volume percent $P_{c/t}$ is $100 \times f_{c/t}$. Note that some authors report $f_{c/t}$ calculations using only one monoclinic reflection in the denominator of eqn. 1, which would result in larger $f_{c/t}$ values.

Results and discussion

The reaction of $ZrCl_4$ with either Na_2O or Na_2O_2 proceeds in a rapid and exothermic manner following initiation with a hot filament (eqn. 2).

$$ZrCl_4 + 2Na_2O_x \rightarrow ZrO_2 + 4NaCl + (x-1)O_2 \qquad x = 1,2 \quad (2)$$

The DSC data from the $ZrCl_4$–$2Na_2O$ reactant mixture shows a small, broad exothermic rise beginning above 100 °C and continuing until a large exothermic event occurs at 300 °C (reaction initiation), which coincides with the sublimation of $ZrCl_4$ ($T_{sub} \approx 320$ °C). This is consistent with other SSM systems where the reaction between precursors becomes rapidly self-propagating near the point where one of the precursors undergoes a phase change, *i.e.* melts, sublimes, or decomposes.[30]

A representative *in situ* temperature measurement of the reaction between $ZrCl_4$ and Na_2O is shown in Fig. 1. The reaction rapidly reaches its maximum temperature of 1354 °C within 0.5 s after initiation. Heat dissipation to the steel reactor causes the reaction to solidify within five seconds as it cools below the melting point of the NaCl byproduct (801 °C). The small isotherm around 800 °C in Fig. 1 is due to NaCl

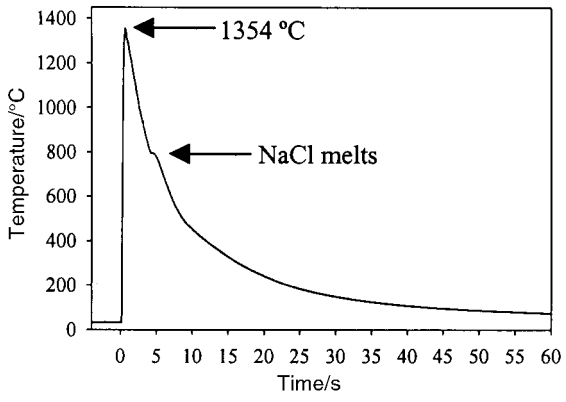

Fig. 1 *In situ* temperature measurements of the reaction between $ZrCl_4$ (4.3 mmol), $2Na_2O$ (8.6 mmol) and 0.1CaO (0.43 mmol). The reaction is initiated by a heated filament at $t = 0$ s.

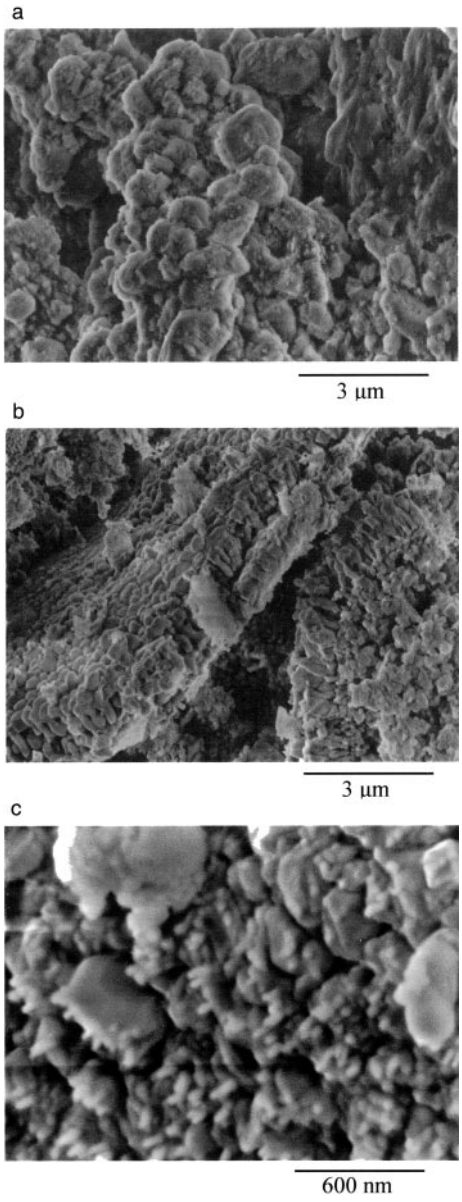

Fig. 2 Scanning electron micrographs of products from the rapid SSM reactions between $ZrCl_4+2Na_2O$ after ethanol workup (a) and after further washing with 2 M HCl (b, c).

solidification. Some of the NaCl is found condensed as beads on cooler regions of the reactor.

A scanning electron micrograph (SEM) of ethanol washed ZrO_2 from the Na_2O reaction shows a smooth, glassy morphology characteristic of a quickly quenched molten salt (Fig. 2a). The water washed product consists of a distribution of smooth, irregularly shaped particles generally less than 500 nm in diameter (Fig. 2b). The dense aligned structures suggest that this SSM reaction proceeds with some directional component. For example, solid-state combustion reactions are often modeled by an oscillating propagation wave front.[31] The pores between elongated features may have contained salt that was washed away. On higher magnification some small diameter (*ca.* 50 nm) rod-like structures are occasionally observed (Fig. 2c). These may be actual crystallites since their diameter is similar to the crystallite size measurements (Table 1).

Powder X-ray diffraction (XRD) data on the acid washed ZrO_2 product demonstrates that it is a crystalline mixture of the thermodynamic room-temperature monoclinic phase (m-ZrO_2) and the high-temperature cubic and/or tetragonal (c/t-ZrO_2) forms (Fig. 3a). The XRD data for the Na_2O_2 reaction is qualitatively similar to the Na_2O results, however less c/t-ZrO_2 is produced. The XRD crystallite sizes are near 30 nm and lattice parameters agree well with literature values (see Table 1). These ZrO_2 mixtures completely convert to the

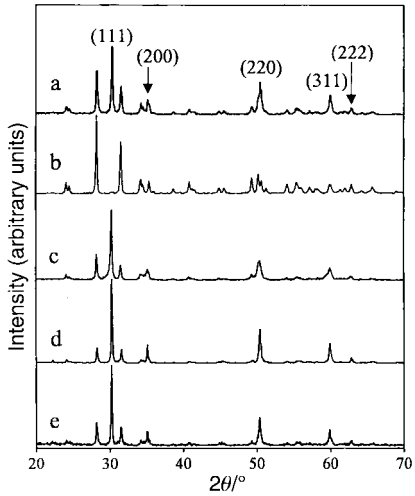

Fig. 3 Powder X-ray diffraction patterns of acid washed products from rapid SSM reaction between $ZrCl_4+2Na_2O$ as-synthesized (a), annealed at 900 °C for 1 day producing pure m-ZrO_2 (b), with 4.5 at% Y_2O_3 added to the reactants (c), with 9 at% CaO added to the reactants (d), and with 9 at% $CaCl_2$ (balanced with Na_2O) added to the reactants (e). The c-ZrO_2 peaks in (a) are indicated by (*hkl*) values.

Table 1 Structural and compositional data for ZrO_2 and HfO_2 products

Sample[a]	Stabilizing additive	Cubic lattice parameter[b] *a*/Å	Cubic crystallite size[c]/nm	Monoclinic crystallite size[c]/nm	Zr(Hf) : M atomic ratio by EDS	$P_{c/t}$/vol%
ZrO_2	n/a	5.107(2)	33	27	n/a	42
ZrO_2 from Na_2O_2	n/a	5.104(3)	27	27	n/a	29
Ca–ZrO_2	CaO	5.113(2)	42	34	96 : 4	71
Y–ZrO_2	Y_2O_3	5.116(2)	33	36	94 : 6[d]	62
Ce–ZrO_2	CeO_2	5.137(3)	26	33	91 : 9	65
CaCl–ZrO_2	$CaCl_2$	5.116(1)	47	30	94 : 6	61
YCl–ZrO_2	YCl_3	5.116(2)	25	32	94 : 6[d]	65
CeCl–ZrO_2	$CeCl_3$	5.134(4)	24	39	87 : 13	47
HfO_2	n/a	5.086(7)	41	42	n/a	9
Ca–HfO_2	CaO	5.100(1)	32	32	95 : 5	43

[a]Na_2O was the oxygen source in all reactions unless otherwise noted. [b]All monoclinic ZrO_2 second phases were within the range: $a=5.14(1)$ Å, $b=5.21(3)$ Å, $c=5.31(1)$ Å, $\beta=99.1(2)^\circ$, which is comparable to literature values.[2,9c] [c]Calculated using $(11\bar{1})_m$, $(111)_m$, and $(111)_{c/t}$ XRD peaks. [d]Determined using cubic lattice parameter and ref. 24*b*, due to Zr and Y peak overlap.

monoclinic structure upon annealing in air at 900 °C for one day (Fig. 3b). Differential thermal analysis of the mixed phase product shows a broad endotherm near 1200 °C corresponding to the monoclinic to tetragonal phase transition (m→t) and a clear exotherm at 970 °C on cooling corresponding to the t→m phase transition. The resulting product had an XRD pattern corresponding to pure m-ZrO_2. The 1200 °C endotherm is more prevalent upon reheating the converted material, consistent with the fact that less m-ZrO_2 was present in the initial heating run.

Phase stabilization with metal oxides

In an effort to stabilize larger fractions of the high-temperature phase(s) to room temperature, 9 at% of known cubic stabilizing oxides (MO_x, where M = Ca, Y, or Ce) were added to the $ZrCl_4$–$2Na_2O$ reactant mixture (eqn. 3). The metal oxides examined are CaO, Y_2O_3, and CeO_2. These stabilizers substitute for Zr^{4+} in the ZrO_2 structure and retard the martensitic phase transformation.

$$ZrCl_4 + 2Na_2O + 0.1MO_x \rightarrow 1.1Zr_{0.91}M_{0.09}O_{1.82+0.09x} + 4NaCl \quad (3)$$

The metal oxide stabilized products will be referred to as Ca–ZrO_2, Y–ZrO_2, and Ce–ZrO_2, respectively. The XRD results show a significant increase in the percentage of the cubic/tetragonal phase (60–70%) relative to the unstabilized product (see Fig. 3c,d and Table 1). Experiments using twice the amount of CaO (Zr : Ca ratio of 5 : 1) showed no further stabilization of the c/t-ZrO_2 phase. Energy dispersive spectroscopy (EDS) shows the presence of substantial amounts of the metal additive in all acid-washed products. Due to peak overlap, the Y–ZrO_2 composition was determined using its cubic lattice parameter, which is known to vary linearly with yttrium subsitution.[24b] Since a small amount of CeO_2 is observed in the XRD of the cerium stabilized product, its composition is an upper limit. The stabilized products show no loss in the c/t-ZrO_2 fraction after heating to 900 °C and only a slight change at 1300 °C where the $P_{c/t}$ drops from 71% to 58% and 62% to 49% for the Ca–ZrO_2 and Y–ZrO_2 materials, respectively. The $P_{c/t}$ decrease suggests that some of the cubic phase consists of unstabilized ZrO_2, however DTA experiments up to 1450 °C on Ca–ZrO_2, Y–ZrO_2, and Ce–ZrO_2 showed no thermal transitions, consistent with significant retardation in monoclinic phase conversion.

SEM images show that these stabilized metathesis products consist of smooth, spherical, agglomerated particles (Fig. 4).

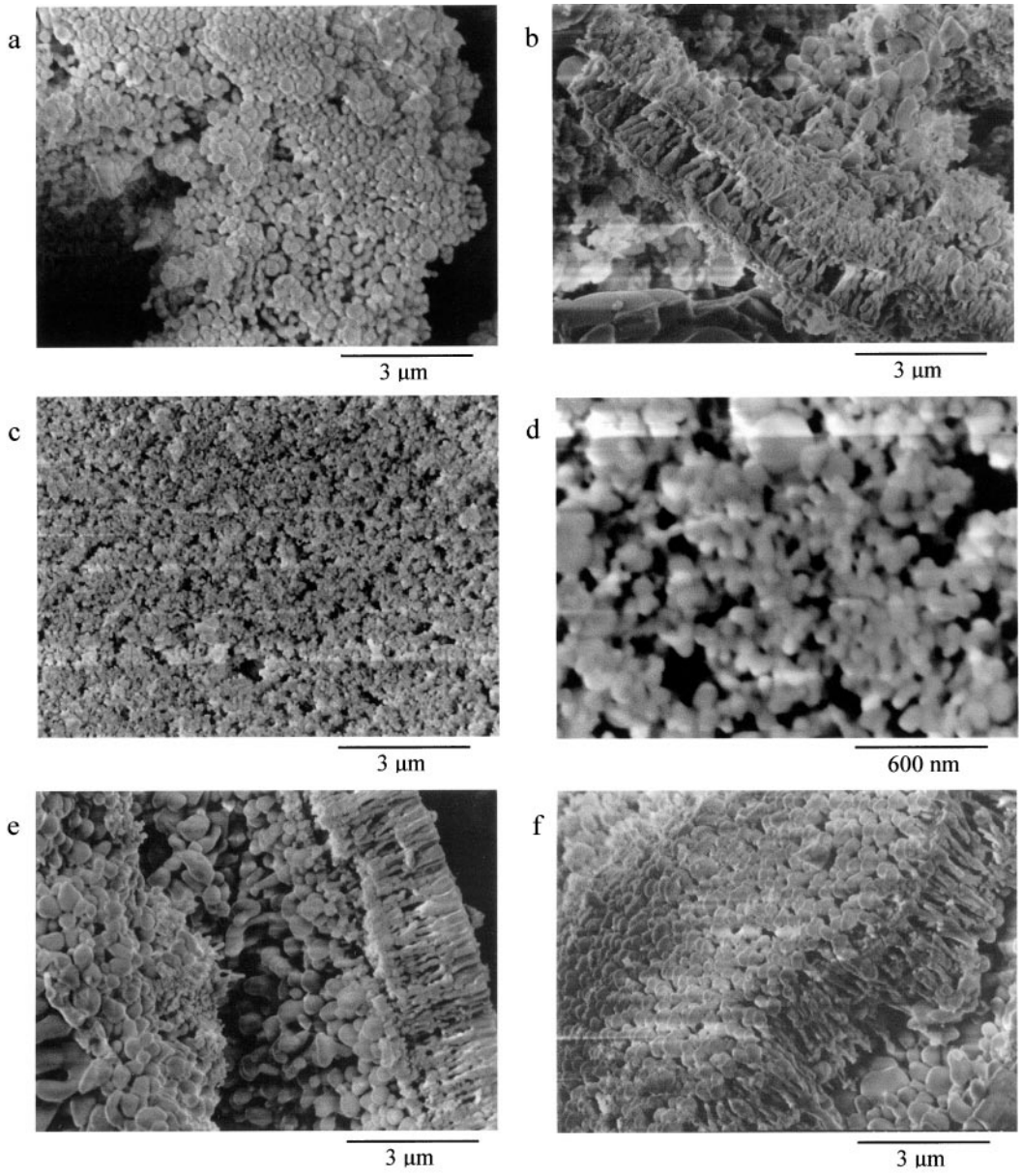

Fig. 4 Scanning electron micrographs of the ZrO_2 products stabilized using CaO (a, b), Y_2O_3 (c, d), $CeCl_3$ (e), and $CaCl_2$ (f).

While XRD results suggest that crystalline domains are comparable for all metal substituted zirconias, the Ca–ZrO_2 (Fig. 4a,b) has much larger particles compared to Y–ZrO_2 (Fig. 4c,d), roughly 300 nm *versus* 100 nm, respectively. In all cases elongated, aligned growth structures are observed in the product, similar to those in Fig. 2b.

Phase stabilization with metal chlorides

Previous SSM studies found that intimate mixtures of metal halides can produce solid-solution products.[32] To test this possibility for cubic ZrO_2, small quantities of a stoichiometric amount of $CaCl_2$, YCl_3, or $CeCl_3$ balanced with Na_2O were added to the $ZrCl_4$–Na_2O reaction (eqn. 4). The zirconium metal ratio (10 : 1) was the same as for the metal oxide additions above.

$$ZrCl_4 + (2+0.05y)Na_2O + 0.1MCl_y \rightarrow 1.1Zr_{0.91}M_{0.09}O_{1.82+0.045y} + (4+0.1y)NaCl \quad (4)$$

Note that the cerium chloride oxidation state (3+) is lower than in the previous case for cerium oxide (4+). The reaction products will be referred to as CaCl–ZrO_2, YCl–ZrO_2, and CeCl–ZrO_2. In each of these reactions the percentage of the c/t-ZrO_2 phase was increased relative to unstabilized ZrO_2 (see Fig. 3e and Table 1). The particle morphologies observed in these systems are similar to those noted above, including indications of long-range features that may be remnants of the SSM propagation wave (Fig. 4e,f). The origin of these ordered structures is under investigation.

Cubic *versus* tetragonal stabilization

Since the transformation of the unit cell from the cubic to tetragonal structure involves only a slight elongation along the c axis (cubic phase: $a = 5.11$ Å; tetragonal phase $a = 5.09$ Å, $c = 5.18$ Å), it is necessary to examine high-angle X-ray lines to distinguish between the cubic and tetragonal phases. The cubic (004) reflection occurs at 74° and is distinct from the tetragonal (004) and (400) reflections at 73° and 74.5°, respectively. Fig. 5 shows the XRD results at high angles (70–80°) for stabilized (Fig. 5b) and unstabilized ZrO_2 (Fig. 5d). Simulated patterns for the cubic, tetragonal, and monoclinic phases are included for comparison (Figs. 5a,c,e). The most intense peaks for m-ZrO_2 are present in both spectra to varying degrees; however, they do not interfere with the region of interest. The c-ZrO_2 (004) peak is prominent in *both* the stabilized and unstabilized ZrO_2, indicating that c-ZrO_2 is formed at temperatures well below its thermodynamic transition temperature (2380 °C).

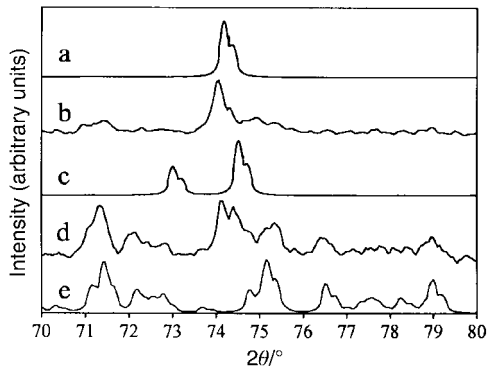

Fig. 5 High angle X-ray diffraction data for a simulated c-ZrO_2 pattern (a), the Ca–ZrO_2 SSM product (b), a simulated t-ZrO_2 pattern (c), the unstabilized ZrO_2 SSM product (d), and a simulated m-ZrO_2 pattern (e).

Hafnia phase stabilization

Hafnium and zirconium have similar sizes and properties and this carries over to their respective oxide phases as well. Rapid SSM reactions between $HfCl_4$ and Na_2O with or without the addition of 9 at% CaO (Ca–HfO_2) result in mixed phase products analogous to the zirconia reactions. However, high-temperature cubic/tetragonal phase stabilization is considerably less than for the comparable ZrO_2 reaction; for example, the unstabilized HfO_2 reaction contains less than 10% of the c/t-HfO_2 phase. SEM analysis shows that HfO_2 and Ca–HfO_2 each consist of smooth, spherical particles with sizes near 150 nm and 300 nm, respectively.

Reaction propagation and product growth

Since the MCl_4 (M = Zr, Hf) reagent is much more volatile (sub. < 350 °C) than the added metal oxides (bp > 2400 °C) or metal chlorides (bp > 720 °C), the stabilized products have the potential to be enriched in the metal additive relative to eqns. (3) and (4). However, a competing effect is that solid-solution stability is usually limited and other metal rich phases may form; for example, $CaZrO_3$ is observed in the ethanol washed Ca–ZrO_2 and CaCl–ZrO_2 products. In addition, since Na_2O is involatile it will remain in the reaction zone, thus forming detectable amounts of Na_2ZrO_3 by XRD. Both of these alkali/alkaline earth phases are readily removed during the acid wash.

These metal oxide SSM reactions are easily initiated and reach high temperatures because of the large exothermic heat of reaction; for example, eqn. (2) has a ΔH_{rxn} of -925 kJ mol^{-1} when Na_2O is used. Rapid SSM reactions are considered as adiabatic processes and thus standard enthalpy values have been used to calculate *theoretical* maximum reaction temperatures (T_{max}).[16,20,31,33] Using this adiabatic assumption, the ZrO_2 ΔH_{rxn} ideally provides enough energy to raise ZrO_2 and the NaCl byproduct to a T_{max} of 1413 °C, the boiling point of NaCl. The experimental *in situ* temperature measurements closely approach this theoretical adiabatic limit (see Fig. 1). The addition of excess NaCl as an inert heat sink to the ZrO_2 SSM reaction, resulting in a 1 : 10 ZrO_2 : NaCl ratio, causes the $P_{c/t}$ to drop to less than 19%. The theoretical adiabatic T_{max} for this SSM reaction with the NaCl additive is calculated to be only 1006 °C. This suggests that the metathesis reaction between $ZrCl_4$ and Na_2O nucleates a cubic phase if the reaction reaches temperatures near the monoclinic–tetragonal phase transition (1205 °C) and is rapidly quenched to room temperature. This is in contrast to previous SSM studies on ZrP where salt additions did not affect the amount of the high-temperature cubic phase.[21] The lower $P_{c/t}$ values for HfO_2 reactions, in general, may reflect the fact that the theoretical T_{max} (still 1413 °C) is well below the equilibrium phase transition temperature (1670 °C).

Conclusions

Solid-state metathesis (SSM) reactions are a useful alternative to conventional high-temperature synthetic methods. They are solvent-free, often exothermic, and once initiated rapidly reach high temperatures and produce crystalline materials in seconds. The only byproducts are alkali salts that are easily washed away. Recently the rapid quenching ability of this SSM route was demonstrated to produce metastable high-temperature phases. This article describes an example of metastable ZrO_2 phase formation using a rapid SSM route. The exothermic metathesis reaction between solid $ZrCl_4$ and Na_2O initiates near the sublimation point of the metal halide, reaches temperatures approaching 1400 °C in a fraction of a second, and quickly cools to room temperature. The washed product is a crystalline mixture of cubic and monoclinic ZrO_2 phases. The

high-temperature cubic ZrO_2 phase may initially nucleate in the hot molten salt and is then quenched before it transforms to the stable monoclinic phase. The addition of cubic stabilizing additives to the ZrO_2 reaction produces larger amounts (up to 70 vol%) of the cubic phase and increases its high-temperature stability. Analogous reactions can be used to produce metastable cubic HfO_2 in either unstabilized or stabilized form. The rapid synthesis/quenching aspects of the SSM method may provide access to complex mixed metal oxides that phase separate under conventional high-temperature reaction conditions. The extension of this method to other metastable binary and mixed metal compounds is under investigation.

Acknowledgements

The authors thank the University of Iowa (E. G. G.) and National Science Foundation (R. B. K.) for financial support.

References

1 W. H. Rhodes and S. Natansohn, *Ceram. Bull.*, 1989, **68**, 1804.
2 R. Stevens, *Zirconia and Zirconia Ceramics*, publication no. 113, Magnesium Elektron Ltd., Manchester, UK, 1986, and references therein.
3 W. D. Kingery, J. Pappis, M. E. Doty and D. C. Hill, *J. Am. Ceram. Soc.*, 1959, **42**, 395.
4 A. H. Heuer, *J. Am. Ceram. Soc.*, 1987, **70**, 689.
5 (*a*) Y. C. Zhang, S. Davison, R. Brusasco, Y. T. Qian, K. Dwight and A. Wold, *J. Less-Common Met.*, 1986, **116**, 301; (*b*) S. Davison, R. Kershaw and A. Wold, *J. Solid State Chem.*, 1988, **73**, 47; (*c*) H. Al Raihani, B. Durand, F. Chassagneux, D. Kerridge and D. Inman, *J. Mater. Sci.*, 1994, **4**, 133.
6 (*a*) R. Srinivasan, M. B. Harris, R. J. De Angelis and B. H. Davis, *J. Mater. Res.*, 1988, **3**, 787; (*b*) V. S. Nagarajan and K. J. Rao, *J. Mater. Sci.*, 1989, **24**, 2140; (*c*) R. P. Denkewicz, Jr., K. S. TenHuisen and J. H. Adair, *J. Mater. Res.*, 1990, **5**, 2698.
7 (*a*) A. Chatterjee, S. K. Pradhan, A. Datta, M. De and D. Chakravorty, *J. Mater. Res.*, 1994, **9**, 263; (*b*) A. Benedetti, G. Fagherazzi and F. Pinna, *J. Am. Ceram. Soc.*, 1989, **72**, 467; (*c*) A. Cimino, D. Gazzoli, G. Minelli and M. Valigi, *J. Mater. Chem.*, 1992, **2**, 75.
8 (*a*) B. E. Yoldas, *J. Am. Ceram. Soc.*, 1982, **65**, 387; (*b*) L. Yang and J. Cheng, *J. Non-Cryst. Solids*, 1989, **112**, 442; (*c*) C. Sanchez and J. Livage, *New J. Chem.*, 1990, **14**, 513; (*d*) D. R. Ulrich, *Chem. Eng. News*, 1990, 28; (*e*) T. J. Bastow, M. E. Smith and H. J. Whitfield, *J. Mater. Chem.*, 1992, **2**, 989.
9 (*a*) R. Srinivasan, R. De Angelis and B. H. Davis, *J. Mater. Res.*, 1986, **1**, 583; (*b*) R. Srinivasan, C. R. Hubbard, O. B. Cavin and B. H. Davis, *Chem. Mater.*, 1993, **5**, 27; (*c*) X. Bokhimi, A. Morales, O. Novaro, M. Portilla, F. Tzompantzi and R. Gomez, *J. Solid State Chem.*, 1998, **135**, 28.
10 (*a*) K. S. Mazdiyasni, C. T. Lynch and J. S. Smith, *J. Am. Ceram. Soc.*, 1966, **49**, 286; (*b*) H. Nishizawa, N. Yamasaki, K. Matsuoka and H. Mitsushio, *J. Am. Ceram. Soc.*, 1982, **65**, 343; (*c*) C. L. Ong, J. Wang, S. C. Ng and L. M. Gan, *J. Am. Ceram. Soc.*, 1998, **81**, 2624.
11 (*a*) R. C. Garvie, *J. Phys. Chem.*, 1965, **69**, 1238; (*b*) A. H. Heuer, N. Claussen, W. M. Kirven and M. Rühle, *J. Am. Ceram. Soc.*, 1982, **65**, 642.
12 A. Chakraborty, P. S. Devi, S. Roy and H. S. Maiti, *J. Mater. Res.*, 1994, **9**, 966.
13 (*a*) N. A. Dhas and K. C. Patil, *J. Mater. Sci. Lett.*, 1993, **12**, 1844; (*b*) N. A. Dhas and K. C. Patil, *J. Solid State Chem.*, 1993, **102**, 440.
14 D. A. Harrison, R. Stevens and S. J. Milne, *J. Mater. Sci. Lett.*, 1987, **6**, 673.
15 (*a*) S. Hilpert and A. Wille, *Z. Phys. Chem. Abt. B*, 1932, **18**, 291; (*b*) B. Durand and J. M. Paris, *Inorg. Synth.*, 1980, **20**, 50; (*c*) A. L. Hector and I. P. Parkin, *Polyhedron*, 1993, **12**, 1855; (*d*) A. L. Hector and I. P. Parkin, *J. Mater. Sci. Lett.*, 1994, **13**, 219; (*e*) A. T. Rowley and I. P. Parkin, *Inorg. Chim. Acta*, 1993, **211**, 77.
16 L. Rao, E. G. Gillan and R. B. Kaner, *J. Mater. Res.*, 1995, **10**, 353.
17 E. G. Gillan and R. B. Kaner, *Inorg. Chem.*, 1994, **33**, 5693.
18 L. Rao and R. B. Kaner, *Inorg. Chem.*, 1994, **33**, 3210.
19 J. B. Wiley, E. G. Gillan and R. B. Kaner, *Mater. Res. Bull.*, 1993, **28**, 893.
20 For reviews of sealed tube and rapid SSM reactions: (*a*) I. P. Parkin, *Chem. Soc. Rev.*, 1996, 199; (*b*) J. B. Wiley and R. B. Kaner, *Science*, 1992, **255**, 1093; (*c*) E. G. Gillan and R. B. Kaner, *Chem. Mater.*, 1996, **8**, 333.
21 R. F. Jarvis, Jr., R. M. Jacubinas and R. B. Kaner, *Inorg. Chem.*, 2000, **39**, 3243.
22 G. L. Kulanski, *J. Am. Ceram. Soc.*, 1968, **51**, 582.
23 (*a*) R. C. Garvie, R. H. Hanink and R. T. Pascoe, *Nature*, 1975, **258**, 703; (*b*) D. J. Green, D. R. Maki and P. S. Nicholson, *J. Am. Ceram. Soc.*, 1974, **57**, 136.
24 (*a*) H. G. Scott, *J. Mater. Sci.*, 1975, **10**, 1527; (*b*) R. P. Ingel and D. Lewis, III, *J. Am. Ceram. Soc.*, 1986, **4**, 325.
25 (*a*) J.-G. Duh, H.-S. Dai and W.-Y. Hsu, *J. Mater. Sci.*, 1988, **23**, 2786; (*b*) V. S. Nagarajan and K. J. Rao, *J. Mater. Res.*, 1991, **6**, 2688.
26 (*a*) M. Yokoyama, T. Ota and I. Yamai, *J. Cryst. Growth*, 1989, **94**, 287; (*b*) G. Tilloca, *J. Mater. Sci.*, 1995, **30**, 1884.
27 (*a*) L.-M. Tau, R. Srinivasan, R. J. De Angelis, T. Pinder and B. H. Davis, *J. Mater. Res.*, 1988, **3**, 561; (*b*) S. Wang, H. P. Li and R. Stevens, *J. Mater. Sci.*, 1992, **27**, 5397.
28 B. E. Warren, *X-Ray Diffraction*, Dover Publications, New York, 1990, pp. 251–258.
29 (*a*) R. C. Garvie and P. S. Nicholson, *J. Am. Ceram. Soc.*, 1972, **55**, 303; (*b*) P. A. Evans, R. Stevens and J. G. Binner, *Br. Ceram. Trans. J.*, 1984, **83**, 39.
30 R. E. Treece, E. G. Gillan and R. B. Kaner, *Comments Inorg. Chem.*, 1995, **16**, 313.
31 (*a*) Z. A. Munir, *Ceram. Bull.*, 1988, **67**, 342; (*b*) Z. A. Munir and U. Anselmi-Tamburini, *Mater. Sci. Rep.*, 1989, **3**, 277.
32 P. R. Bonneau and R. B. Kaner, *Inorg. Chem.*, 1993, **32**, 6084.
33 (*a*) H. C. Yi and J. J. Moore, *J. Mater. Sci.*, 1990, **25**, 1159; (*b*) R. M. Jacubinas, TMAX Fortran program, Ph.D. Dissertation, Dept. of Chemistry, University of California, Los Angeles, 1995.